

<sup>1</sup>. Branislav DOBRUCKY, <sup>2</sup>. Mariana BENOVA, <sup>3</sup>. Slavomir KACSAK

## ANALYSIS OF LCTL C RESONANT CONVERTER QUANTITIES FOR DIFFERENT OUTPUT

<sup>1,3</sup>. DEPARTMENT OF MECHATRONICS AND ELECTRONICS, UNIVERSITY OF ZILINA, SLOVAKIA

<sup>2</sup>. DEPARTMENT OF OF ELECTROMAGNETIC AND BIOMEDICAL ENGINEERING, UNIVERSITY OF ZILINA, SLOVAKIA

**ABSTRACT:** The paper deals with design analysis, simulation, synthesis and verification of power resonant converter integrated with LCLC filter, HF transformer and rectifying output. The output voltage of LCTL C in the basic AC direct mode is sinusoidal one with harmonic distortion roughly 5% in the whole range of the load with possibility of non-symmetrical control of the converter. A novel detailed analysis of over-loaded rectifying mode with DC output is given, as well as transfer and transient properties analysis, non-linearity including. Simulations based on Matlab/OrCad models confirmed by experimental results of both modes are given in the paper.  
**KEYWORDS:** resonant-mode power supplies, DC/AC converters, LCLC resonant filter

### INTRODUCTION

One of the progressive alternative, by which it is able to reach requested parameters of high power density, high efficiency and with low EMI/EMC influence, is LLC resonant converter topology ([13]-[15], [7]). These converters are developed and manufactured since 90's and their topology has many advantages [13], [14].

Nowadays, targeting increase of power density and efficiency, the new topologies of resonant converters are being developed [1], [2], [6], [7], [13]-[16]. Even those topologies consist of more resonant components compared to LLC converter. The magnetic components can be integrated and can have small dimensions as well as low consumption. These structures, upgraded with parallel resonant circuit and with synchronous MOSFET rectifier operated in inverse regime, can achieve efficiency of 95,5 % with power density of 95W/in<sup>3</sup> and switching frequency up to 2,3 MHz [1], [13]. A LCTL C resonant converter can provide both types of AC or DC power supply, and it is usually used as power supply for either HV rectifiers (vacuum displays and CRTs, [2], X-ray devices [8] or fluorescent lamps [1], or HF cycloconverters or matrix converters [11]).

### BASIC TOPOLOGY OF LCTL C INVERTER

The basic scheme of LCTL C resonant inverter is shown in Figure 1.

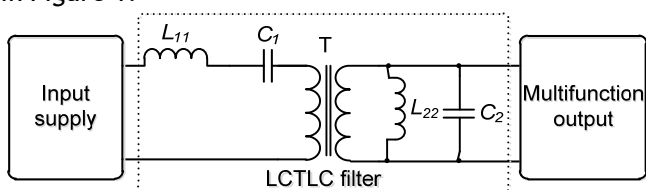


Figure 1. Block scheme of LCTL C resonant inverter

It consists of input supply, LC series resonant filter (with parameters  $L_{11}$  and  $C_1$ ), HF transformer (HV or normal MV), and LC parallel resonant filter ( $L_{22}$  and  $C_2$ ) and multifunction output. The HF transformer can also be connected after the LCLC filter, if necessary.

#### A. Input supply possibilities

Basically, input supply of the LCTL C can be considered by three ways, i.e.: a) full-bridge DC-AC inverter, b) half-bridge one with centre type of the DC source, c) DC-DC buck converter.

#### B. Multifunction output possibilities

Output of LCTL C can be loaded by simply RL load - direct AC output or rectified RL load - rectified DC output, respectively, Figure 2a, b or AC output with variable or constant frequency LV, Figure 2c. Other possibility is connecting of cycloconverter or matrix converter to the LCTL C.

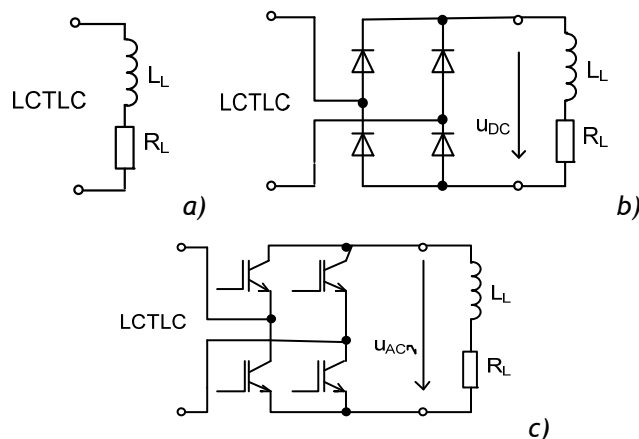


Figure 2. Basic connections of LCTL C output  
 C) Proposed connection of LCTL C resonant inverter  
 The basic scheme of proposed LCTL C resonant inverter is shown in Figure3. It consists of DC/DC buck converter, LC series resonant filter (with

parameters  $L_{11}$  and  $C_1$ ), HF transformer (HV or normal MV), and LC parallel resonant filter ( $L_{22}$  and  $C_2$ ). The HF transformer can also be connected after the LCLC filter, if necessary.

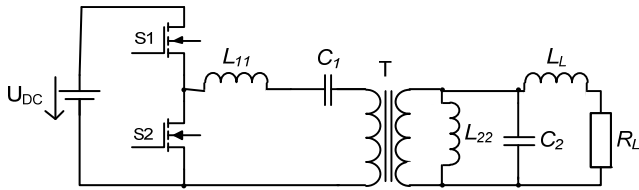


Figure 3. Basic scheme of proposed LCTLC resonant inverter

**DIRECT AC OUTPUT MODE ANALYSIS OF LCTLC INVERTER**

The following analysis is oriented, contrary to [2], [17] on design analysis of LCLC components, investigation of transfer- and transient properties, and also influence of non-linearity of inductors. Since the input voltage of LCTLC  $u_1(t)$  involves certain DC component voltage this component has been omitted due to series capacitor, and investigated circuit are supposed to be supply by AC rectangular voltage Figure4.

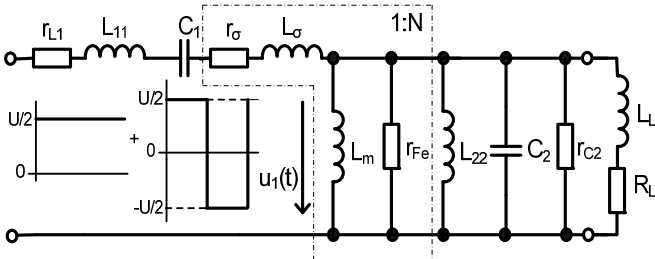


Figure 4. Equivalent scheme of LCTLC circuit with R-L load

The parameters of the HF transformer [2], [17] are included into resulting component parameters, and then:

$$R_1 = R_{l1} + R_{\sigma} \tag{1a}$$

$$\frac{1}{R_2} = \frac{1}{R_{Fe}} + \frac{1}{R_{22}} \tag{1b}$$

$$L_1 = L_{11} + L_{\sigma} \tag{1c}$$

$$\frac{1}{L_2} = \frac{1}{L_m} + \frac{1}{L_{22}} \tag{1d}$$

State-space model equation

$$\frac{di_{L1}}{dt} = \frac{r_1}{L_1} i_{L1} - \frac{1}{L_1} u_{C1} - \frac{1}{L_1} u_{C2} + \frac{1}{L_1} u_1; \tag{2a,b}$$

$$\frac{di_{L2}}{dt} = \frac{1}{L_1} u_{C2}; \frac{du_{C1}}{dt} = \frac{1}{C_1} i_{L1};$$

$$\frac{du_{C2}}{dt} = \frac{1}{C_2} i_{L1} - \frac{1}{C_2} i_{L2} - \frac{1}{r_2 C_2} u_{C2} - \frac{1}{C_2} i_{LL}; \tag{2d,e}$$

$$\frac{di_{LL}}{dt} = -\frac{R_L}{L_L} i_{LL} + \frac{1}{L_L} u_{C2}$$

Using suitable numerical method or directly Matlab functions the time waveforms of the quantities of LCTLC inverter can be obtained, Figure 5.

When input  $U_{DC}$  voltage is varying then RMS value of fundamental harmonic will be also varied. To be

constant the asymmetric control of duty cycle of S1, S2 has to be provided [9], [12].

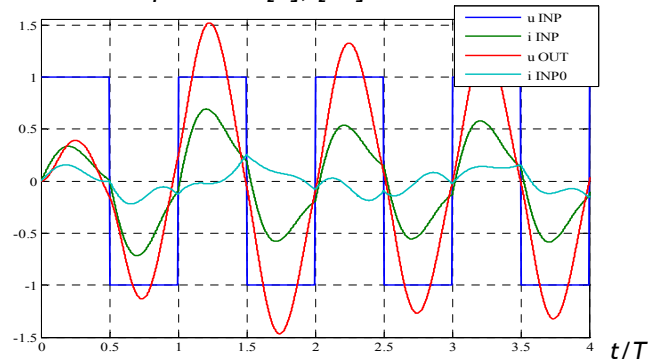


Figure 5. Simulated waveforms of LCTLC inverter (p.u.)

**A) LCLC Elements Design Synthesis Criteria**

From the different point of view one can obtain:

- minimum voltage and current stress of the storage elements in the steady-state  $|Z_{L1,2}| = |Z_{C1,2}|$ ;  $q = 1$
- minimum total harmonic distortion:  $THD < 5\%$  (we need to know the impedance frequency characteristic)
- minimum voltage and current stress of the accumulate elements in transient states (we need transient analysis).

Resonant frequency of  $L_1$ ,  $C_1$  and  $L_2$ ,  $C_2$  should be the same as basic fundamental frequency of the converter and is requested by load demands. So, based on Thomson relation [18]

$$\omega_{res} = \sqrt{\frac{1}{L_1 C_1}} = \sqrt{\frac{1}{L_2 C_2}}$$

or, respectively

$$L_1 \omega_{res} = \frac{1}{\omega_{res} C_1} = L_2 \omega_{res} = \frac{1}{\omega_{res} C_2} \tag{3}$$

where  $\omega_{res}$  is equal  $2\pi$  times fundamental frequency of the converter. Theoretically,  $\omega_{res} L_1$  and other members of (3) can be chosen from wide set. Not to exceed nominal voltages and currents of the accumulative elements we take value of the nominal load  $|Z_L|$ . Then where  $q_1, q_2$  quality factors are ratio of impedance of components  $L_1, C_1$  or  $L_2, C_2$  to the nominal load impedance.

$$L_1 = \frac{U_1^2}{\omega_{res} P_1} q_1, \quad C_1 = \frac{P_1}{\omega_{res} U_1^2} \frac{1}{q_1} \tag{4}$$

$$L_2 = \frac{U_2^2}{\omega_{res} P_2} \frac{1}{q_2}, \quad C_2 = \frac{P_2}{\omega_{res} U_2^2} q_2$$

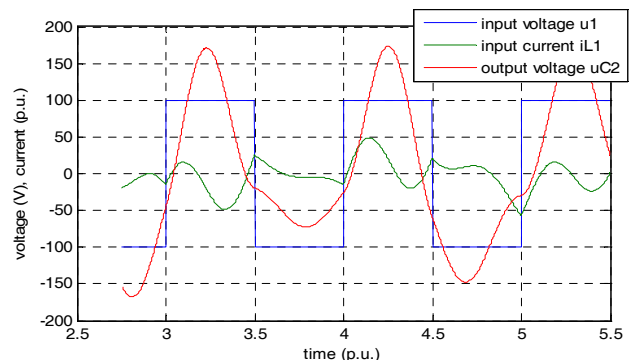


Figure 6. Output voltage of LCLC under load disconnection in the middle of half period [18]

**B) Transient analysis of LCTL**

Analysis was done in works [4], [9]. Transient phenomena were simulated for two sets of filter parameter values: basic values of the filter parameters (i.e. quality factor  $q$  ( $Q$ ) of the filter equal one), and for quality factor equal two, when resonant reactances ( $\omega_{res}L$ ) and capacitances ( $1/\omega_{res}C$ ) are equal 2-multiply of the nominal load  $|Z_N|$ , Figure 6. It is possible to simulate transient phenomena with considering non-linear function  $L = f(i_L)$  as is shown in [5].

As can be seen in Figure 6 for  $q_1 = 0.6$  and  $q_2 = 1$  the over voltage during load disconnect is +7.5 % regarding to maximum value of output voltage in steady-state only. By selecting appropriate values of quality factors  $q_1, q_2$  the voltage stresses can be minimized ( $<U_{Mnom} + 5\%$ ).

Voltage transfer characteristic of LCLC filter  $U_2/U_1$  (Bode diagram) is shown in Figure 7.

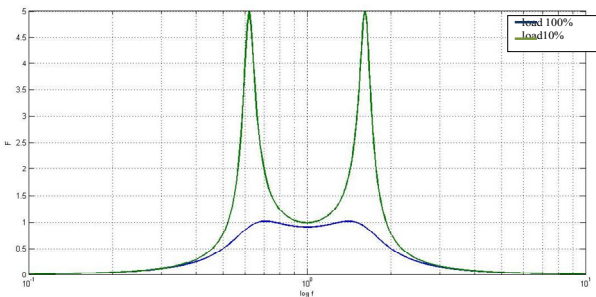


Figure 7. Voltage transfer characteristic of LCLC filter  $U_2/U_1$

The output voltage at equality of  $\omega_{res}$  and  $\omega_{sw}$  is almost constant; small difference is caused by voltage drop on passive resistances of inductor  $L_1$  and capacitor  $C_1$ .

**C) Experimental verification of direct AC output mode**

Basic measurement of input and output voltages of the LCTL under no load are shown in Figure 8, with following parameters:  $L_1 = 14.61 \mu H$ ;  $L_2 = 14.61 \mu H$ ;  $C_1 = 99 nF$ ;  $C_2 = 99 nF$ ;  $U = 6.00 V$ ;  $r_1 = 0.1 \Omega$ ;  $r_2 = 20 k\Omega$ ;  $f = 132 kHz$ ;  $R_L = 12.25 \Omega$  (full load);  $L_L = 174 \mu H$

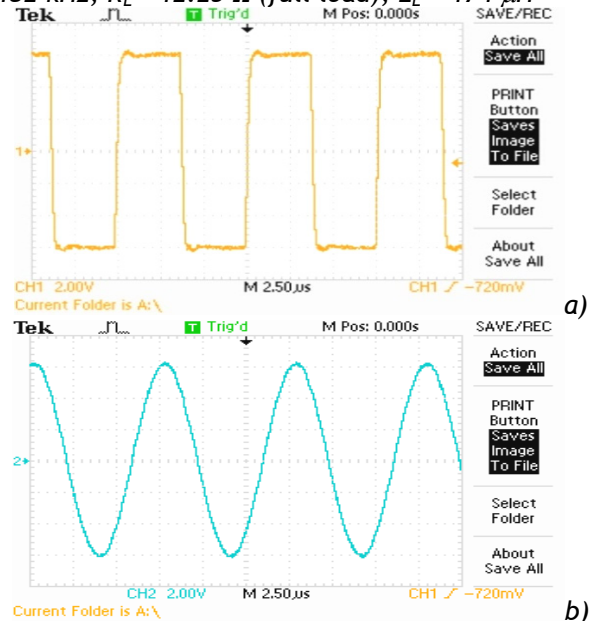


Figure 8. Experimental input and output voltages in no-load operation. a) input voltage; b) output voltage

**Used apparatus and devices:**

- Signal generator Agilent 33521 30 MHz;
- Power linear amplifier Krohn-Hite 7500;
- Transformer used: Type Flyback;
- $P_{out} = 2 W$ ;  $f_T = 132 kHz$ ;  $L_\sigma = 0.6 \mu H$ ;
- $U_{1,2} = 5 - 15 V_{rms}$ ; ( $N_1/N_2 = 1:1$ )
- Settings:  $U_1 = 6 V$ ;  $f_{sw} = 132 kHz$ .

Results of measurement of input and output voltages and input current of the LCTL are shown in Figure 9.

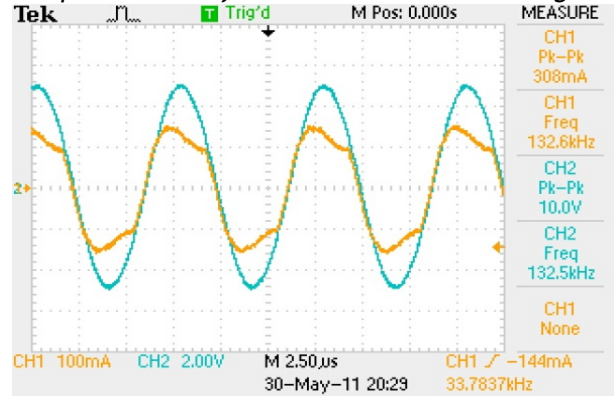


Figure 9. Experimental results: input and output voltage under full load

Since the output quantities are in good agree with simulation ones, the input voltage is due to non-zero impedance of DC source only 4.4 V (average value) under full load instead 6 V at no-load.

**CURRENT RECTIFYING DC OUTPUT MODE**

There are four different topologies for LCTL with output rectifier A); B); C); D), Figures 10, 11, 12, 13 for extended analysis in overcurrent loading rectifier mode.

**Topology for positive half-period of input voltage and positive rectified output**

A)  $U_{C2}$  is positive and grater than threshold voltages of  $D_1, D_4$  diodes, Figure 10.

Since  $u_{C2}$  voltage is positive ( $> 2U_{Th}$ ) then all equations (2a) - (2e) are valid. As a consequence of resonant phenomena in the circuitry the  $u_{C2}$  voltage will cross zero level when current  $i_{C2}$  charges capacitor having negative polarity:

$$i_{C2} = i_{LL} - (i_{L1} - i_{L2}) \quad (5)$$

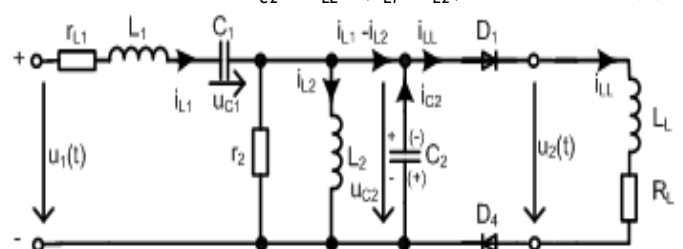


Figure 10. Diagram for positive half-period of input voltage and positive rectified output

B)  $U_{C2}$  is negative and greater than diode threshold voltages of  $D_2, D_3$  diodes, Figure 11

When the  $u_{C2}$  voltage becomes negative the  $D_2, D_3$  diodes are opening and therefore Eqs. (2d), (2e) will be changed into (6a,b):

$$\frac{du_{C2}}{dt} = \frac{1}{C_2} i_{L1} - \frac{1}{C_2} i_{L2} - \frac{1}{r_2 C_2} u_{C2} + \frac{1}{C_2} i_{LL} \quad (6a)$$

$$\frac{di_{LL}}{dt} = -\frac{R_L}{L_L} i_{LL} - \frac{1}{L_L} u_{C2} \quad (6b)$$

That means the  $C_2$  capacitor will be overcharged by inductors energy back to positive polarity.

$$i_{C2} = i_{LL} + (i_{L1} - i_{L2}) \quad (7)$$

To be negative again (and voltage too) sum of the currents  $i_{L1}$ ,  $i_{LL}$  and has to be negative one. When the sum on the right side is zero, the capacitor current  $i_{C2}$  becomes zero (and voltage  $u_{C2}$  too).

$$\text{if } i_{L2} \geq i_{LL} + i_{L1} \text{ then } i_{C2} \leq 0 \quad (8)$$

The process can be repeating periodically until fulfilling of above condition or can be finish after one period depending on inductors energies. These circumstances are depicted in Figure 12.

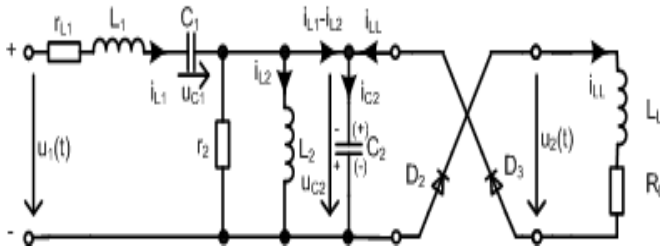


Figure 11. Positive half-period but negative  $u_{C2}$  voltage

After fulfilling of condition (8) the  $i_{L2}$  current stays nearly constant (see both Figures 12a and 12b). Interesting is that during steady-state the ‘zero voltage’ period will be placed symmetrically to  $T/2$ -axis (see Figures 15a,b and 16b).

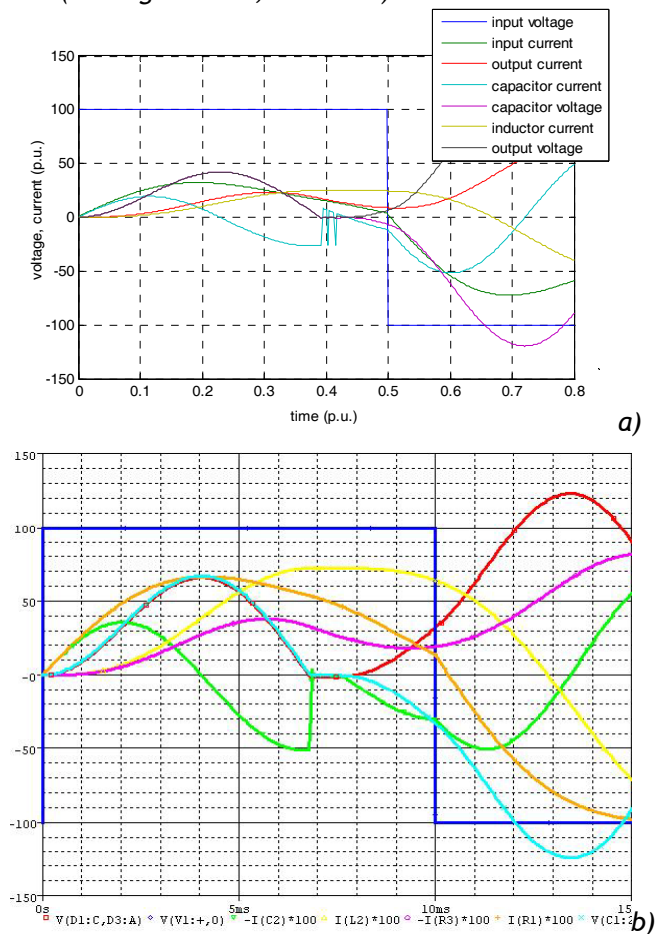


Figure 12. Time waveforms during  $u_{C2}$  crossing zero a) using MatLab, b) using OrCAD environment

**Topology for negative half-period of input voltage and positive rectified output**

The similar processes will be doing during negative half-period of input voltage.

C)  $U_{C2}$  is negative and greater then threshold voltages of  $D_2, D_3$  diodes

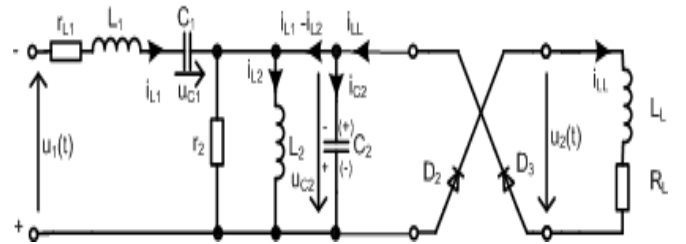


Figure 13. Diagram for negative half-period of input voltage and positive rectified output

D)  $U_{C2}$  is positive and greater then diode threshold voltages, Figure 14.

The length of zero rectified voltage depends on following factors:

- loading of the rectifier; greater load cause longer zero voltage
- ratio of  $L_L$  and  $L_2$  inductances (parameter of LCTL circuit)
- value of  $i_{L1}$  at instant of  $u_{C2}$  voltage zero crossing
- time constant of the load (ratio  $L_L/R_L$ )

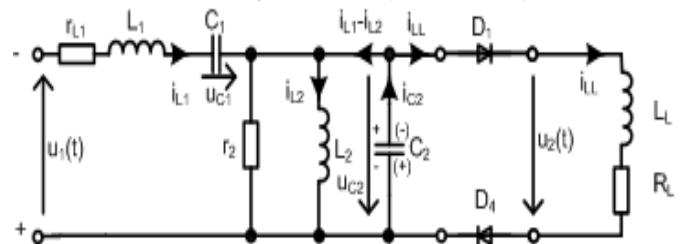


Figure 14. Negative half-period but positive  $u_{C2}$  voltage

Note that ‘zero voltage’ period can also occur under normal operation of LCTL depending on its parameters, and almost always during overloading. On other hand, the mechanism causing ‘zero voltage’ has also a benefit: it restricts overcurrent due to decreasing of output rectified voltage average value as shown in Figures 15a,b and 16b.

**Experimental Verification of Extended Analysis in Overcurrent Loading Rectifier Mode of LCTL**

Following parameters have been used for simulation and experimentation:  $L_1 = L_2 = 14.60 \mu H$ ;  $C_1 = C_2 = 99 \text{ nF}$ ;  $R_L = 12.25 \Omega$ ;  $L_L = 174 \mu H$

Transformer used: Type Flyback  $P_{out} = 2 \text{ W}$ ;  $f_T = 132 \text{ kHz}$ ;  $L_\sigma = 0.6 \mu H$ ;  $U_{1,2} = 5 - 15 \text{ V}_{rms}$ ;  $(N_1/N_2 = 1:1)$

Signal generator type of: Agilent 33521 30 MHz

Power linear amplifier type: Krohn-Hite Model 7500

Schottky diodes BAT 41:  $0.45 \text{ V}/T_j = 25^\circ \text{C} (1\text{V}/200 \text{ mA})$   
Settings:  $U_1 = 5 \text{ V}$ ,  $f_{sw} = 132 \text{ kHz}$ ,  $R_L = 12.25 \Omega$  (full load) -  $6.15 \Omega$  (2-fold overloading).

There are shown overloading waveforms in Figures 15a and 15b - simulation, and in Figure 16b - experimental verification, at steady-states with nominal R-L load ( $\cos\varphi = 0.8$ ).

Verification of rectifier mode at steady-states with pure resistive load is presented in Figure 16a.

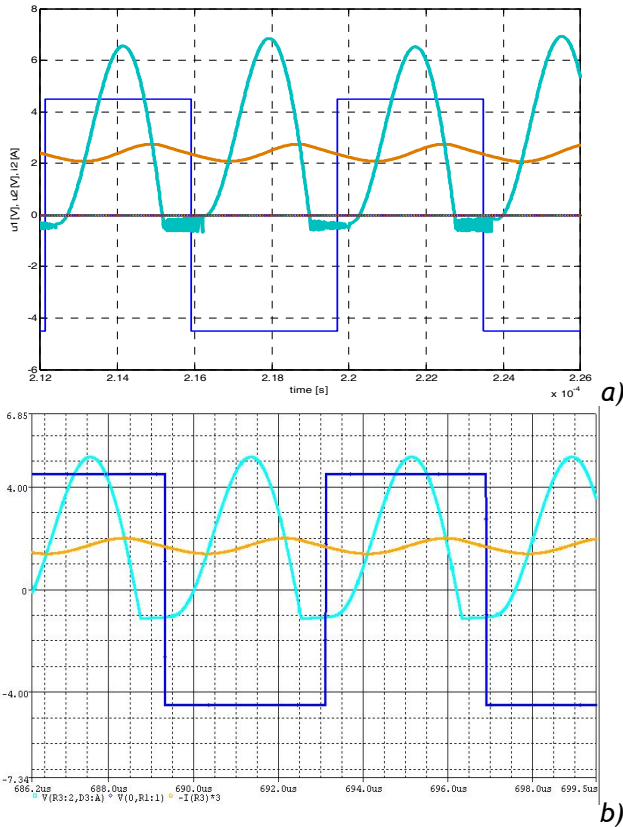


Figure 15. Simulation experiments for overloaded rectifier mode: in Matlab (a) and OrCad (b) environment

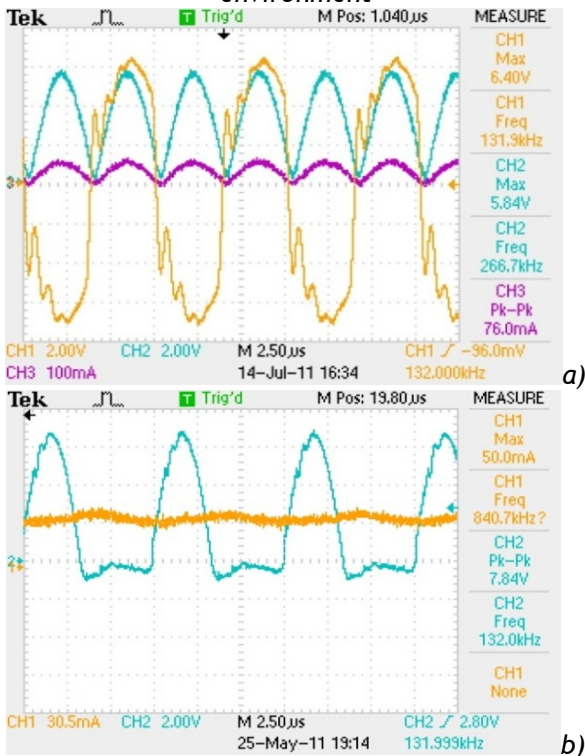


Figure 16. Rectifier mode under R load (a)- and overloaded rectifier mode under R-L load (b) of LCTLc - oscilloscope view

As one can see from achieved results the output voltage is not constant but depends on value and character of the load. Using asymmetrical control [9], [12] is possible to control of output voltage or to hold it on constant value. Dependency of fundamental harmonic of  $u_1(t)$  input voltage on

control angle  $\beta$  or duty cycle, respectively is given by relation:

$$\frac{U_1(\beta)}{U} = \frac{\sqrt{2}}{\pi} \sqrt{1 - (\cos(\beta)) \dots} (= \frac{2}{\pi} \sin(\frac{\beta}{2})) \quad (9)$$

where control angle  $\beta$  is equivalent to the width of pulse.

The voltage (its fundamental harmonic) is then transformed through the resonant LC circuit to the output of LCTLc converter. Using simply control voltage loop the output can be regulated in the range from zero up to maximum value ( $2/\pi \cdot U_{DC} \cdot N_1/N_2$ ; where  $N_1/N_2$  is transformer ratio).

Using controlled rectifier with MOSFETs instead of Schottky diodes could be also possible a classical phase shift control.

Another way how to control of output voltage is to use voltage transfer function of LCTLc which gain depends on used switched frequency - that means: frequency control.

**CONCLUSIONS**

There has been described in the paper two modes of LCTLc converter:

- direct AC (HF) mode,
- rectifying DC mode (with output SD or MOSFET rectifier).

At the first one the LCTLc converter with HF output mode is used as power supply source of high frequency voltage for industrial applications (e.g. hardening of materials, demagnetisation in bearing production). Quality of the output voltage is very high, total harmonic distortion can be lesser than 5%. The second mode of LCTLc uses Schottky diode or MOSFET rectifier for DC output. This mode with Schottky diode was intensively analysed in the paper mainly regarding to overloading when occurring ‘zero voltage’ period in output voltage.

Both modes are verified by Matlab ‘equational’ simulation, OrCad circuit simulation, and by experimental testing with good results. The analysis results showed very good transfer and also functional properties of LCTLc:

- output voltage is stable and constant, practically independent on the loading,
- during overloading a ‘zero voltage’ period is generated; output voltage decreasing, and consequently output current is restricted.

**Acknowledgment**

The authors wish to thank for the financial support to the CEX 2 R&D operational program Centre of excellence of power electronics systems and materials for their components II. No. OPVaV-2009/2.1/02-SORO, ITMS 26220120046 funded by European regional development fund (ERDF) and Slovak Research and Development Agency APVV project No. APVV-0138-10.

**REFERENCES**

[1.] Ang, Y.A.; Stone, D.A.; Bingham, C.M.; Foster, M.P.: Rapid Analysis & Design Methodologies of High-Frequency LCLC Resonant Inverter as Electrodeless Fluorescent Lamp Ballast. In: Proc. of IEE-PEDS’07 Int’l Conf., pp. 139-144, 2007.

- [2.] Ang, Y.A.; Foster, M.P.; Bingham, C.M.; Stone, D.A.; Sewell, H.I.; Howe, D.: Analysis of 4th-Order LCLC Resonant Power Converters. In: Proc. of IEE Electrical Power Applications, Vol. 131, No. 2, pp.169-181, 2004.
- [3.] Batarseh, I.: Resonant Converter Topologies with Three and Four Storage Elements. In:IEEE Transaction on Power Electronics, Vol. 9, No.1, pp. 64-73, 1994.
- [4.] Benova, M.; Dobrucky, B.: Methodological Approach to Steady-State and Transient Investigation of Electric Circuits using Numerical Infinite Series of Two-Phase System. In: Electrical Review, (PL), Vol. LXXXVII, No. 5, pp. 6-8, 2011.
- [5.] Benova, M.; Dobrucky, B.; Pokorny, M.: Non-Linear Modeling and Simulation of High Order Resonant Filter - Inverter System in Transient and Steady States. In: Proc. of ASM'11 Int'l Conf., Crete (GR), pp. CD-ROM, 2011.
- [6.] Borage, M.; Tiwari, S.; Kotaiah, S.: Analysis and Design of an LCL-T Resonant Converter as a Constant-Current Power Supply. In: IEEE Trans. on Industrial Electronics, Vol. 52, No. 6, pp. 1547-1554, 2005.
- [7.] Castilla, M.; de Vicuna, L.G.; Guerrero, J.M.; Matas, J.; Miret, J.: Sliding-Mode Control of Quantum Series-Parallel Resonant Converters via Input-Output Linearization. In: IEEE Trans. on Industrial Electronics, Vol. 52, No. 2, pp. 566-575, 2005.
- [8.] Cavalante, S.F.: High Output Voltage Series-Resonant DC-DC Converter for Medical X-Ray Imaging Applications. In: Dissertation No. 16414, ETH Zurich (CH), 2006.
- [9.] Dobrucky, B.; Benova, M.; Kascak, S.: Transient Analysis and Modelling of 2nd- and 4th-Order LCLC Filter under Non-Symmetrical Control. In: Electronics and Electrical Engineering (LT), Vol. 5 (111), pp. 89-94, 2011.
- [10.] Dobrucky, B.; et al.: Two-Phase Power Electronic Drive with Split - Single- Phase Induction Motor. In: Proc. of IECON'10 Int'l Conf., IEEE-IES, Phoenix (AZ, USA), pp. CD-ROM, 2010.
- [11.] Dobrucky, B.; Benova, M.; Kascak, S.: Design Analysis of LCLC Resonant Inverter for Two-Stage 2-Phase Power Electronic Supply System. In: Automatika- Journal of Control, Measurement, Electronics, Computing and Communications, ISSN 0005-1144, 2012 (paper accepted).
- [12.] Imbertson, P.; Mohan, N.: Asymmetrical Duty-Cycle Permits Zero Switching Loss in PWM Circuits with No Conduction Loss Penalty. In: IEEE Trans. on Industry Applications, Vol. 29, No. 1, 1993.
- [13.] Lee, F.C.; et al.: Power Architecture Design with Improved System Efficiency, EMI and Power Density. In: Proc. of IEEE-PESC'08 Int'l Conf., Rhodes (GR), pp. 4131-4137, 2008.
- [14.] Lee, F.C.; Wang, S.; Kong, P.; Wang, C.; Fu, D.: Technology Trends toward a System-in-a-Module in Power Electronics. In: IEEE Circuits and Systems Magazine, Vol. 2, Issue 4, pp. 4-22, 2002.
- [15.] Lucia, O.; Burdío, J.M.; Millan, I.; Acero, J.; Puyal, D.: Load-Adaptive Control Algorithm of Half-Bridge Series Resonant Inverter for Domestic Induction Heating. In: IEEE Trans. on Industrial Electronics, Vol. 56, No. 8, pp. 3106-3116, 2009.
- [16.] Peng, Y.F.; Wai, R.-J.; Lin, Ch. M.: Implementation of LLC-Resonant Driving Circuit and Adaptive CMAC Neural Network Control for Linear Piezoelectric Ceramic Motor. In: IEEE Trans. on Industrial Electronics, Vol. 51, No. 1, pp. 35-48, 2004.
- [17.] Radvan, R.; Dobrucky, B.; Frivaldsky, M.; Rafajdus, P.: Modelling and Design of HF 200 kHz Transformers for Hard- and Soft- Switching Application. In: Electronics and Electrical Engineering, KTU Kaunas (LT), Vol. 4 (110), pp. 7-12, 2011.
- [18.] Williams, A. B.; Taylor, F. J.: Electronic Filter Design Handbook. Mac Graw-Hill Inc., Third Edition, ISBN 0-07-070441-4, 1995.



ACTA TECHNICA CORVINIENSIS - BULLETIN OF ENGINEERING



ISSN: 2067-3809 [CD-Rom, online]

copyright © UNIVERSITY POLITEHNICA TIMISOARA,  
FACULTY OF ENGINEERING HUNEDOARA,  
5, REVOLUTIEI, 331128, HUNEDOARA, ROMANIA  
<http://acta.fih.upt.ro>